Lgl mediates apical domain disassembly by suppressing the PAR-3–aPKC–PAR-6 complex to orient apical membrane polarity

Tomoyuki Yamanaka[1,2,*,‡], Yosuke Horikoshi[1,*], Natsuko Izumi[1,2], Atsushi Suzuki[1], Keiko Mizuno[1] and Shigeo Ohno[1,§]

[1]Department of Molecular Biology, Yokohama City University, Graduate School of Medical Science, 3-9 Fuku-ura, Kanazawa-ku, Yokohama 236-0004, Japan
[2]Kihara Memorial Yokohama Foundation for the Advancement of Life Sciences, 1-7-29, Suehiro-cho, Turumi-ku, Yokohama 230-0045, Japan

*These authors contributed equally to this work
‡Present address: Laboratory for Structural Neuropathology, RIKEN Brain Science Institute, 2-1 Hirosawa, Wako, Saitama, 351-198, JAPAN
§Author for correspondence (e-mail: ohnos@med.yokohama-cu.ac.jp)

Accepted 1 February 2006
Journal of Cell Science 119, 2107-2118 Published by The Company of Biologists 2006
doi:10.1242/jcs.02938

Summary

The basolateral tumor suppressor protein Lgl is important for the regulation of epithelial cell polarity and tissue morphology. Recent studies have shown a physical and functional interaction of Lgl with another polarity-regulating protein machinery, the apical PAR-3–aPKC–PAR-6 complex, in epithelial cells. However, the mechanism of Lgl-mediated regulation of epithelial cell polarity remains obscure. By an siRNA method, we here show that endogenous Lgl is required for the disassembly of apical membrane domains in depolarizing MDCK cells induced by Ca^{2+} depletion. Importantly, this Lgl function is mediated by the suppression of the apical PAR-3–aPKC–PAR-6 complex activity. Analysis using 2D- or 3D-cultured cells in collagen gel suggests the importance of this suppressive regulation of Lgl on the collagen-mediated re-establishment of apical membrane domains and lumen formation. These results indicate that basolateral Lgl plays a crucial role in the disassembly of apical membrane domains to induce the orientation of apical membrane polarity, which is mediated by the suppression of apical PAR-3–aPKC–PAR-6 complex activity.

Supplementary material available online at
http://jcs.biologists.org/cgi/content/full/119/10/2107/DC1

Key words: Epithelial cell polarity, Lgl, PAR, Apical membrane domain

Introduction

Lethal giant larva (Lgl), one of the basolateral tumor suppressor proteins in *Drosophila* (Gateff, 1978), has been shown to be an indispensable protein for the establishment of apical-basal polarity of *Drosophila* epidermis and epithelial-derived neural progenitor cells (Bilder et al., 2000; Ohshiro et al., 2000; Peng et al., 2000). In mammals, mammalian homologues of Lgl (mLgl), mLgl-1 and mLgl-2, have also been shown to localize to the basolateral membrane domain of epithelial cells (Musch et al., 2002; Yamanaka et al., 2001). In addition, mLgl-1 knockout mice have been reported to show hyperproliferation of neuroepithelial cells in the developing brain (Klezovitch et al., 2004), suggesting that mLgl is also important for the regulation of epithelial tissue morphology and brain development in mammals.

An apical protein complex containing atypical PKC (aPKC), PAR-6 and PAR-3, the PAR-3–aPKC–PAR-6 complex, has also been shown to be involved in the establishment of apical-basal polarity of epithelial cells (Bilder, 2004; Knust and Bossinger, 2002; Macara, 2004; Ohno, 2001). In *Drosophila*, this protein complex localizes to the subapical regions, and is indispensable for the establishment of apical junctions and apical-basal membrane polarity (Muller and Wieschaus, 1996; Petronczki and Knoblich, 2001; Wodarz et al., 2000). In mammalian epithelial cells, this protein complex localizes to the apical junctions (Hirose et al., 2002; Izumi et al., 1998; Joberty et al., 2000; Lin et al., 2000; Suzuki et al., 2001) and has an important role in the establishment of apical junctions during cell-cell adhesion-mediated epithelial cell polarization (Chen and Macara, 2005; Gao et al., 2002; Hirose et al., 2002; Mizuno et al., 2003; Suzuki et al., 2002; Suzuki et al., 2001; Yamanaka et al., 2001).

Recently, a direct interaction between basolateral Lgl and apical aPKC–PAR-6 complex has been shown in *Drosophila* and mammalian epithelial cells (Betschinger et al., 2003; Hutterer et al., 2004; Yamanaka et al., 2003). In addition, Lgl has been shown to be phosphorylated by aPKC, which is required for the process to exclude Lgl from apical region in epithelial cells (Betschinger et al., 2003; Hutterer et al., 2004; Musch et al., 2002; Yamanaka et al., 2003). On the contrary, in mammalian cells, overexpressed mLgl competes with PAR-3 for its interaction with the aPKC–PAR-6 complex and suppresses the cell-cell adhesion-induced formation of apical junctions in mammalian epithelial cells (Yamanaka et al., 2003). A genetic study using *Drosophila* has shown that a reduction in aPKC levels suppresses the development of Lgl mutant phenotypes, such as cell polarity defects and tumorigenesis (Rolls et al., 2003). Further, studies using

Drosophila or *Xenopus* embryo indicate that mutual inhibition between apical aPKC and basolateral Lgl is important for the maintenance of epithelial membrane polarity (Chalmers et al., 2005; Hutterer et al., 2004). Although these observations suggest the importance of an antagonistic interaction of Lgl with apical PAR-3–aPKC–PAR-6 complex on the development of polarized membrane domains in epithelial cells, the precise mechanism of Lgl-mediated regulation of membrane domain polarization remains obscure.

Using small interfering RNA (siRNA), we provide evidence that endogenous mLgl facilitates the disassembly of apical membrane domains in MDCK cells depolarized by Ca^{2+}-depletion. Importantly, this effect is mediated by the suppression of apical PAR-3–aPKC–PAR-6 complex activity. Furthermore, analyses using 2D- or 3D-cultured MDCK cells in collagen gel suggest that this mLgl-mediated suppression of apical protein complex activity is important for the collagen-mediated orientation of apical membrane polarity.

Results

mLgl knockdown suppresses the disassembly of apical membrane proteins in MDCK cells in response to depolarization

To examine the mechanism of Lgl-mediated regulation of epithelial cell polarity, we initially established MDCK cell clones (24-15 and 24-16) in which both mLgl-1 and mLgl-2 were stably knocked down (mLgl kd), by using pSUPER-based siRNA vectors. Control clones (21-1 and 21-7) were similarly established, by using a negative control sequence. Western blot analysis revealed that the expression of mLgl-1 or mLgl-2 was reduced to less than 10% in both (24-15 and 24-16) clones compared with the 21-1 clone (Fig. 1A). The expression of other proteins including PAR-3, aPKCλ, PAR-6β and PAR-1b was not affected (Fig. 1A).

Since we have shown previously that the overexpression of mLgl-2 in MDCK cells inhibits the formation of apical junctions induced by cell-cell adhesion (Yamanaka et al., 2001), we first performed a Ca^{2+}-switch assay to assess the role

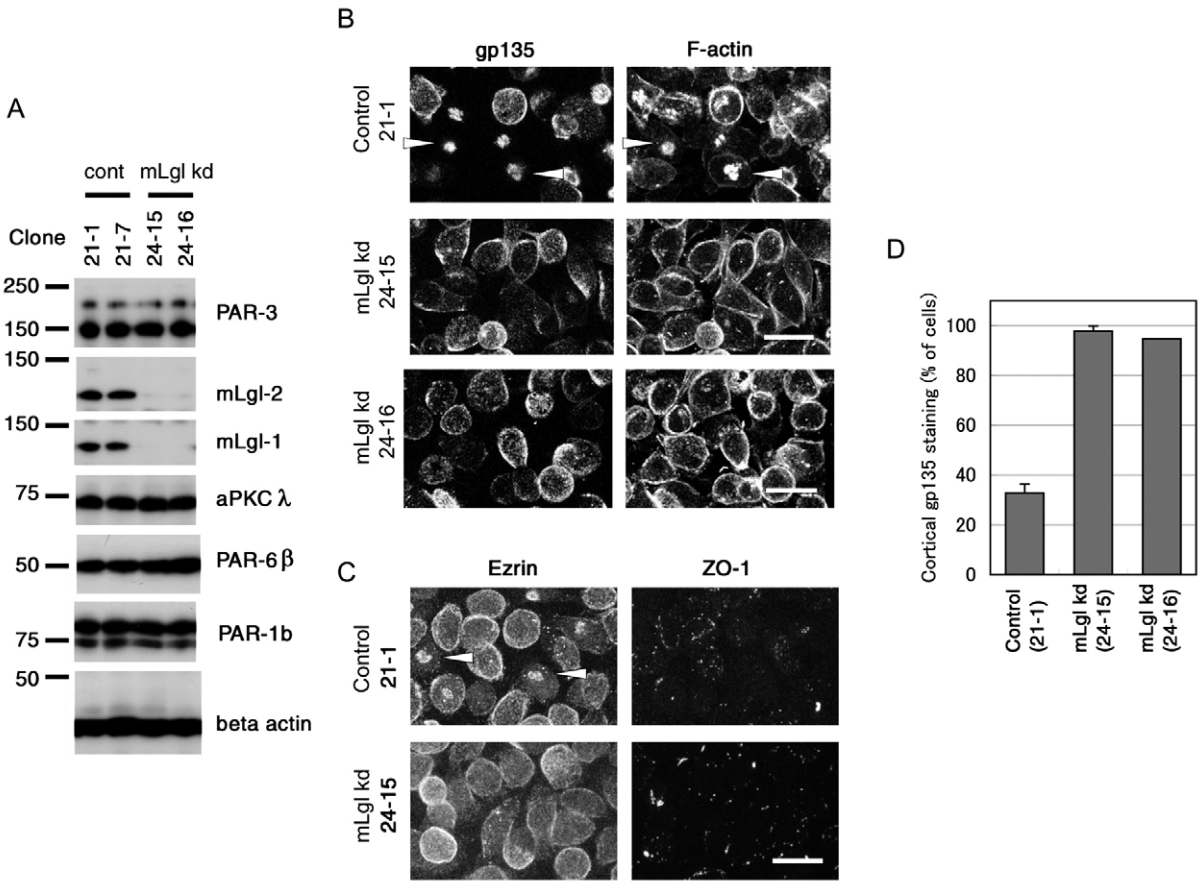

Fig. 1. Knockdown of mLgl retains apical proteins and F-actin at cell periphery in depolarized MDCK cells. (A) Western blot analysis of control cells (21-1 and 21-7) and mLgl-1–mLgl-2 double-kd MDCK cell clones (24-15 and 24-16) with antibodies against indicated proteins. mLgl-1 and mLgl-2 expression levels were specifically reduced in clones 24-15 and 24-16. The mLgl knockdown retains the apical proteins and F-actin at the cell periphery in depolarized MDCK cells. (B) Confluent monolayer of control cells or mLgl kd cells on permeable filter were incubated with LC medium for 20 hours, after which cells were fixed and co-stained with anti-gp135 antibody and Rhodamine-phalloidin. Arrowheads indicate cells with intracellular gp135 and F-actin staining. (C) Cells treated as in B, stained with antibodies against ezrin and ZO-1. Arrowheads indicate cells with intracellular ezrin staining. (D) Quantification of the cells with peripheral gp135 staining. The percentage of total cells is shown. Values are mean (±s.d.) of three independent experiments (21-1 and 24-15) or mean of two independent experiments (24-16). Each photograph represents the projected views of optical sections from the apical to the basal membranes of cells. Bars, 20 μm.

of mLgl-1 and/or mLgl-2 in the formation of epithelial cell polarity initiated by cell-cell adhesion. However, ZO-1 (tight junction), ezrin (apical) and E-cadherin (basolateral) localized almost normally in the mLgl kd cells 3 and 24 hours after the Ca^{2+} switch (supplementary material Fig. S1), suggesting that mLgl is dispensable for the repolarization process of 2D-cultured MDCK cells that was initiated by cell-cell adhesion. Alternatively, the remaining mLgl-1 and mLgl-2 levels might be sufficient for the repolarization process of MDCK cells induced by the Ca^{2+} switch in mLgl kd cells.

By contrast, the most prominent effects of mLgl knockdown were detected in depolarized MDCK cells. As reported previously (Vega-Salas et al., 1987; Vega-Salas et al., 1988), incubation of control cells (21-1) with Ca^{2+}-depleted culture medium induced reductions in levels of the peripheral apical proteins gp135 and ezrin, as well as F-actin, and then redistributed them into intracellular compartments, called vacuolar apical compartments (VACs) (Fig. 1B,C). Importantly, in both mLgl kd cells (24-15 and 24-16) the redistribution of these proteins into VACs was markedly suppressed. Most of the mLgl kd cells retained the apical proteins and F-actin at the cell periphery and intracellular apical proteins were hardly detectable (Fig. 1B,C). Quantification analysis revealed that approxymately 100% of the mLgl kd cells retained gp135 at the cell periphery, compared with only 33% of the control cells (Fig. 1D). In addition, staining of aggregated ezrin was decreased in both mLgl kd cells (Table 1). These results indicate that endogenous mLgl is required for the disassembly of apical membrane proteins and their subsequent redistribution into VACs in response to depolarization of MDCK cells. By contrast, overexpression of human Lgl-2, which has two mismatched bases in the siRNA sequence used for knockdown of canine Lgl-2, decreased the peripheral apical proteins in depolarized mLgl kd cells as well as in control cells (supplementary material Fig. S2A,B), supporting the positive role of mLgl in the disassembly of apical proteins in MDCK cells.

To obtain further insights into the formation of abnormal phenotypes in mLgl kd cells, we analyzed the initial process of depolarization induced by Ca^{2+}-depletion. In this experiment, the localization of apical-surface gp135 was monitored by prelabeling it with an antibody against the extracellular region of gp135. In the control cells, surface gp135 gradually disappeared from the cell cortex and localized to the intracellular regions 5 hours after Ca^{2+}-depletion. F-actin gradually coaggregated with gp135 in the intracellular regions (arrowheads in Fig. 2A,B). Notably, in mLgl-kd cells, gp135 and F-actin remained at the cell cortex even 5 hours after Ca^{2+}-depletion. These results suggest that mLgl is required for the internalization of apical membrane proteins during the depolarization of MDCK cells. Interestingly, the disappearance of ZO-1 and occludin from the cell-cell contact region was partially suppressed in the mLgl-kd cells after Ca^{2+}-depletion (supplementary material Fig. S3). This implies the involvement of mLgl in the disassembly of apical junctions in addition to apical membrane proteins during the depolarization of MDCK cells.

mLgl knockdown increases the amount of PAR-3 that interacts with the aPKC–PAR-6 complex in MDCK cells

We have previously shown that overexpressed mLgl-2 antagonizes the interaction of PAR-3 with the aPKC–PAR-6 complex in epithelial cells (Yamanaka et al., 2001). Thus, we next examined whether the knockdown of endogenous mLgl affects the amount of the PAR-3–aPKC–PAR-6 ternary complex in MDCK cells. The amount of PAR-3 co-precipitated with anti-PAR6β antibody from polarized MDCK cells increased 1.5-fold in both mLgl kd cells (24-15 and 24-16) (Fig. 3A-D), supporting the hypothesis that endogenous mLgl competes with PAR-3 for aPKC–PAR-6 binding in MDCK cells. The amount of aPKC in PAR-6β immunoprecipitates was not affected by mLgl knockdown (Fig. 3A-D), which is consistent with the idea that aPKC and PAR-6 form a stable complex independently of mLgl. Thus, endogenous mLgl has a suppressive effect on the formation of the PAR-3–aPKC–PAR-6 ternary complex in epithelial cells.

Interestingly, mLgl knockdown also caused a marked increase in the co-precipitation of endogenous Cdc42 with PAR-6β, which was hardly detected in the control cells (Fig. 3A). These results suggest that endogenous mLgl not only prevents the aPKC–PAR-6 complex from associating with PAR-3, but also suppresses the interaction of Cdc42 with PAR-6β. It should be noticed that no co-precipitation of Rac1 with PAR-6β was detected (Fig. 3A), suggesting that the Lgl knockdown specifically stabilized the interaction of PAR-6β with Cdc42. Taken together with our previous observation that Cdc42 activates aPKC through PAR-6 in vitro (Yamanaka et al., 2001), these results imply that mLgl also regulates aPKC activity in the aPKC–PAR-6 complex, in addition to its interaction with PAR-3 in epithelial cells.

Table 1. The effects of PAR-3- or mLgl-knockdown on ezrin staining in depolarized MDCK cells

Clones	Staining of aggregated ezrin (number of cells)	Total number of cells	%*
21-1 (control)	184	553	33.2%
24-15 (mLgl kd)	14	465	3.0%
24-16 (mLgl kd)	9	422	2.1%
11-10 (control)	165	573	28.8%
13-32 (PAR-3 kd)	278	545	51.0%
13-33 (PAR-3 kd)	280	586	47.8%

Depolarized MDCK clones were stained with anti-ezrin antibody as described in the legend of Figs 1C and 4C.
*, % of cells that show staining of aggregated ezrin.

mLgl facilitates disassembly of apical membrane proteins by suppressing the activity of the PAR-3–aPKC–PAR-6 complex

To examine whether the mLgl-mediated disassembly of apical membrane proteins results from the suppression of PAR-3–aPKC–PAR-6 complex activity in MDCK cells, we examined the effects of PAR-3 knockdown on the distribution of apical proteins in depolarized MDCK cells. For this purpose, we established the PAR-3-knockdown (PAR-3 kd) clones (13-32, 13-33). Control clones (11-10, 25-2) were similarly established by using a negative control sequence. Western blot analysis revealed that the expression level of PAR-3 in the PAR-3 kd cells decreased to 10% (13-32) or 30% (13-33) compared with the control cells (11-10), whereas the expression levels of other proteins including mLgl-1, mLgl-2, aPKCλ, PAR-6β and PAR-1b were unchanged (Fig. 4A).

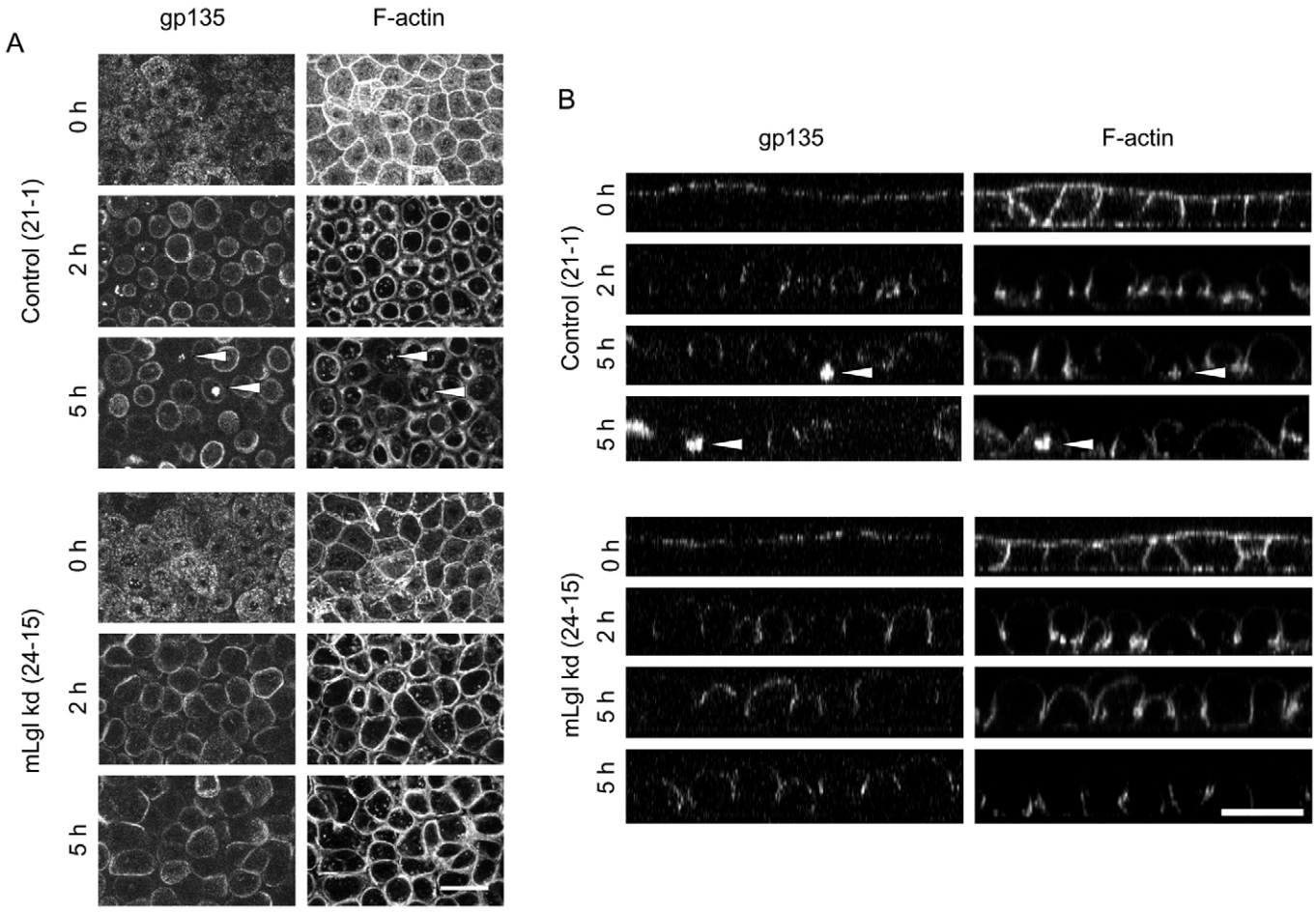

Fig. 2. Knockdown of mLgl suppresses disassembly of apical proteins during the depolarization of MDCK cells. Confluent monolayers were incubated with mouse anti-gp135 antibody for 1 hour. After washing out the antibody, the cells were incubated with LC medium for the indicated time. The cells were fixed, permeabilized and stained with Alexa Fluor 488-conjugated anti-mouse IgG together with Rhodamine-phalloidin. (A) Projected views of optical sections from the apical to the basal membranes of cells. (B) Confocal *z*-sections. Arrowheads indicate cells with intracellular gp135 and F-actin staining. Bars, 20 μm.

Interestingly, PAR-3 kd cells showed opposite phenotypes compared with mLgl kd cells: gp135, ezrin and F-actin levels were decreased in the cell periphery but were increased in the intracellular regions in PAR-3 kd cells (Fig. 4B,C). Quantification analysis revealed that only approximately 10% of cells retained gp135 at the cell periphery in both PAR-3 kd clones (Fig. 4D), whereas staining of aggregated ezrin was increased in these cells (Table 1). Similar results were also obtained from another PAR-3 kd clone (25a) which was established by using other siRNA sequences (supplementary material Fig. S2C,D). By analyzing the initial depolarizing process induced by Ca^{2+}-depletion, we showed that, in contrast to mLgl kd cells, intracellular localization of surface gp135 from the cell periphery was enhanced in PAR-3 kd cells (Fig. 5A,B). Quantification analysis revealed that aggregated gp135 staining was increased by around sixfold in PAR-3 kd cells after incubation with LC medium for 5 hour (Fig. 5C). These results suggest that the PAR-3 knockdown facilitates the disassembly of apical proteins and redistribution of these proteins into the intracellular regions possibly through the enhanced internalization of apical membrane proteins. Thus, endogenous PAR-3 has suppressive effects on the disassembly of apical proteins. By contrast, the overexpression of PAR-3 induced the retention of the peripheral apical proteins in depolarized MDCK cells (supplementary material, Fig. S2C,D), supporting the negative role of PAR-3 in the disassembly of apical proteins in MDCK cells.

In addition, the overexpression of a dominant-negative mutant of aPKC showed a similar phenotype to PAR-3 kd cells in depolarized MDCK cells: only 20% of cells expressing dominant-negative aPKCλ had peripheral gp135 staining, whereas approximately 40% of cells expressing LacZ or wild-type aPKCλ showed peripheral gp135 staining (Fig. 6A,B). Importantly, the overexpression of dominant-negative aPKCλ antagonized the effect of the mLgl knockdown on the redistribution of apical proteins. Overexpression of dominant-negative but not wild-type aPKCλ in mLgl kd cells reduced the number of cells with peripheral gp135 staining to 47% (Fig. 6A,B). These results indicate that aPKC activity also plays a role in suppressing the disassembly of apical proteins during the depolarization process, and mLgl counterbalances this aPKC activity to facilitate apical protein disassembly. Taken together, these data support the notion that mLgl suppresses PAR-3–aPKC–PAR-6 complex activity to facilitate the

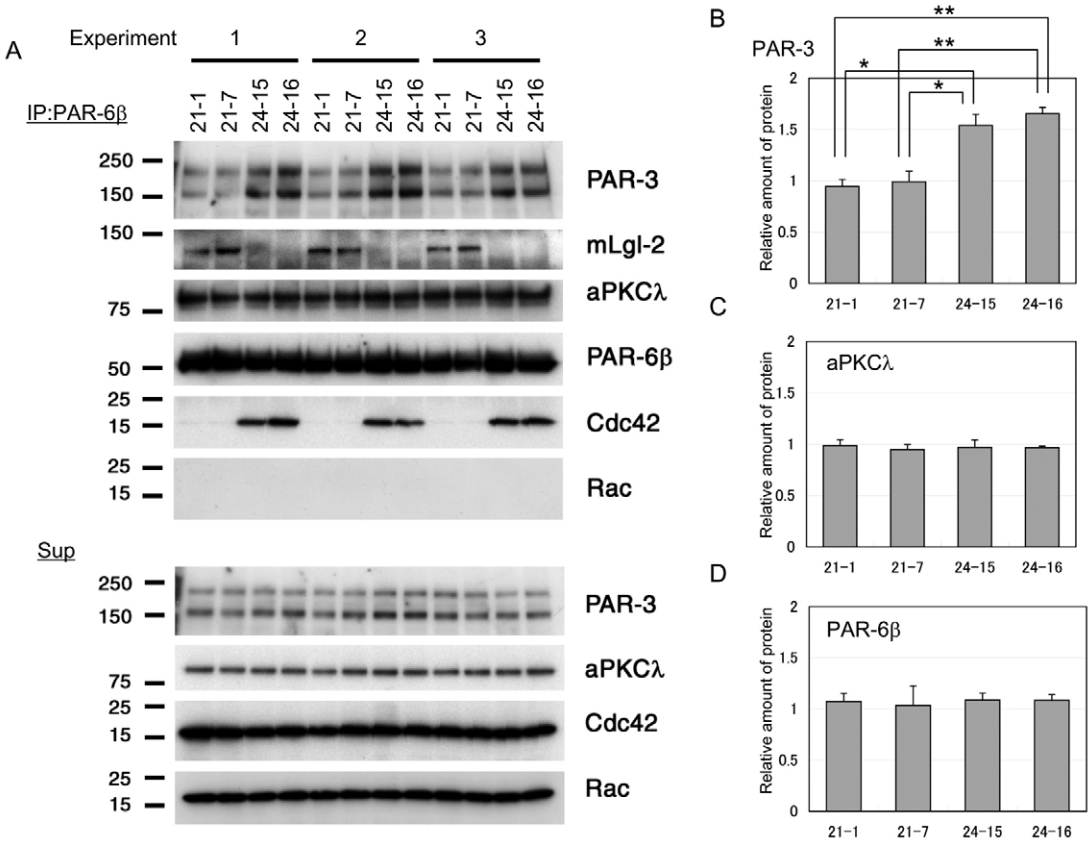

Fig. 3. Knockdown of mLgl increases interaction of aPKC–PAR-6 with PAR-3 or Cdc42. (A) Confluent monolayer of control cells (21-1 or 21-7) or mLgl kd cells (24-15 or 24-16) was lysed with lysis buffer and clarified by centrifugation. The supernatant fraction (Sup, lower panels) containing total 1 mg protein was subjected to immunoprecipitation with anti-PAR-6β antibody and precipitated proteins were analyzed by western blot (IP, upper panels). Three independent experiments were performed for each clone and numbered as 1, 2 and 3. Notice that the co-precipitation of PAR-3 or Cdc42 with PAR-6 was increased in mLgl kd cells. (B-D) Quantification of the amount of PAR-3 (B), aPKCλ (C) or PAR-6β in IP fraction. The amount of PAR-3 increased significantly in both mLgl kd cells (*P<0.005, **P<0.001), whereas the amount of aPKCλ or PAR-6β was not changed in these cells.

disassembly of apical membrane proteins during depolarization of MDCK cells.

mLgl knockdown suppresses re-establishment of apical domains at intracellular regions in response to collagen-gel overlay

It should be noticed that VACs have characteristics of cortical apical membrane domains, that is, they display microvilli and apical protein markers and exclude basolateral proteins (Vega-Salas et al., 1987; Vega-Salas et al., 1988). In addition, VACs do not contain incorporated apical proteins but newly synthesized proteins (Gilbert and Rodriguez-Boulan, 1991). Thus, the above data raise the possibility that mLgl has an important role not only in the disassembly of but also on the re-establishment of de novo apical membrane domains in MDCK cells. To test this, we performed a collagen-gel overlay assay. When MDCK cells cultured sparsely on collagen-coated glass were overlaid with collagen gel, apical domains and apical junctions disappeared, after which de novo apical domains surrounded by apical junctions, called intercellular lumens, were re-established at the intercellular regions (Ojakian et al., 1997; Ojakian et al., 2001; Schwimmer and Ojakian, 1995).

After 24-48 hours of incubating the control cells with collagen gel, the gp135 staining was reduced at the free surface and was detected at the intercellular regions with ZO-1 ring-like staining as previously described (Fig. 7A,B, control cells) (Ojakian et al., 1997). The degree of E-cadherin staining at cell-cell contact regions were also reduced but not diminished completely, as described previously (Fig. 7A) (Ojakian et al., 2001). Interestingly, in mLgl kd cells, the disappearance of gp135 and ZO-1 staining from the free surface and their relocalization at the intercellular regions was markedly suppressed (Fig. 7A). Thus, endogenous mLgl is required for the re-establishment of apical domains in response to collagen-gel overlay.

By contrast, PAR-3 kd cells overlaid with collagen gel showed opposite phenotypes to mLgl-kd cells. Although PAR-3 kd cells induced the formation of intercellular lumens similarly to the control cells at 24 hours after collagen-gel overlay (Fig. 7B,C), at an early stage, the population of colonies with lumens was increased in PAR-3 kd cells. At 10.5 hours after collagen-gel overlay, more than 80% of the colonies of PAR-3 kd cells were positive for intercellular gp135 staining, whereas only 20% of the colonies of the control cells were positive for the staining (Fig. 7B,C). Thus, PAR-3

knockdown accelerated the collagen-gel-mediated re-establishment of apical domains, suggesting a negative role of endogenous PAR-3 in the re-establishment of apical domains. This is in contrast to the role of mLgl, supporting the notion that mLgl facilitates the collagen-mediated re-establishment of intercellular apical domains by counterbalancing PAR-3 function.

mLgl knockdown suppresses orientation of apical membrane polarity and lumen formation during MDCK cystogenesis in collagen gel

In vivo, apical-basal polarity of epithelial cells is subjected to dynamic regulation during tissue development and morphogenesis. The above results imply that mLgl exerts a similar role in the various physiological processes that reorganize apical-basal polarity. To evaluate this, we examined the effect of mLgl knockdown on MDCK cell cystogenesis. When MDCK cells were cultured in a collagen-I gel, the cells proliferated, acquired an apical-basal polarity and finally created cysts with a single lumen at a central position (O'Brien et al., 2002). It has been suggested that collagen-mediated interaction of cell with extracellular matrix (ECM) is important for the orientation of apical membrane polarity; perturbation of this step resulted in inversion of apical membrane polarity and induction of cell aggregate formation without an obvious lumen (O'Brien et al., 2001; Yu et al., 2005).

We first examined the effects of mLgl knockdown on the establishment of apical membrane domains during the early phases of cystogenesis (days 2-3). In this experiment, two independent mLgl kd cells (#1 and #2) and control cells were established by using an autonomous replication siRNA vector, pEB6-SUPER (see Materials and Methods). As described previously (O'Brien et al., 2002), in control cysts, gp135 staining was detected only at the inner surfaces of the cysts (Fig. 8), and concentrated F-actin staining was detected at these inner surfaces (Fig. 9A, days 2-3). Notably, in cysts of mLgl kd cells, gp135 staining was detected at the outer surfaces of the cysts (Fig. 8), and concentrated F-actin staining at inner surfaces was not detected (Fig. 9A, days 2-3). These data suggest that mLgl knockdown suppresses the distribution of apical proteins in the inner surfaces of cysts, resulting in the formation of cysts with inverted apical membrane polarity. It

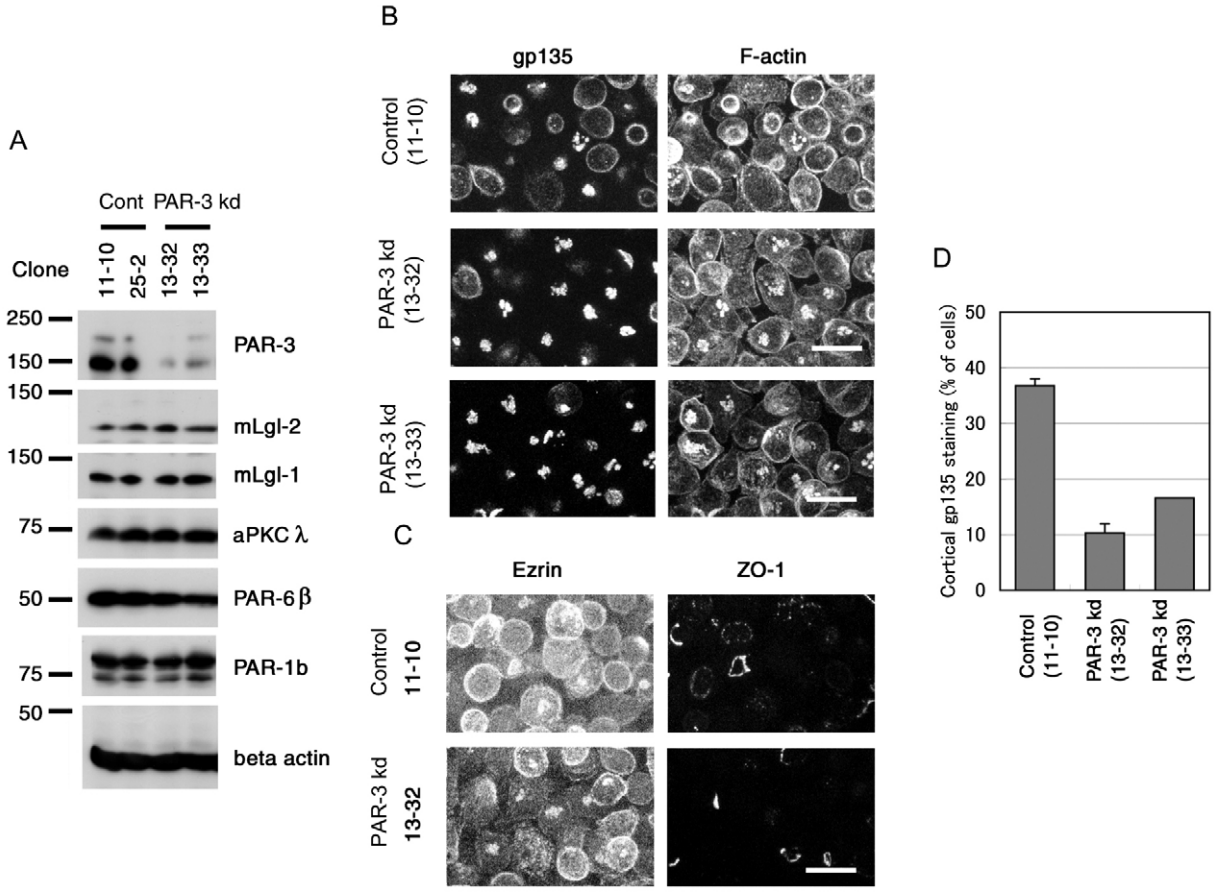

Fig. 4. PAR-3 knockdown decreases peripheral apical proteins in depolarized MDCK cells. (A) Western blot analysis of control cells (11-10 and 25-2) and PAR-3 kd cells (13-32 and 13-33) with antibodies of indicated proteins. Notice that the PAR-3 expression level was specifically reduced in clones 13-32 and 13-33. (B) A confluent monolayer of each cell on a permeable filter was incubated with LC medium for 20 hours, after which the cells were fixed and co-stained with anti-gp135 antibody and Rhodamine-phalloidin. (C) Cells treated as in B, stained with antibodies against ezrin and ZO-1. (D) Quantification of cells with cell peripheral gp135 staining. The percentage of total cells is shown. Values are mean (±s.d.) of three independent experiments (11-10 and 13-32) or mean of two independent experiments (13-33). Each photograph represents the projected views of optical sections from the apical to the basal membranes of cells. Bars, 20 μm.

should be noticed that the basolateral proteins, β-1 integrin and E-cadherin, were detected in the entire cell periphery including the cell-cell contact regions and outer surfaces of cysts of mLgl kd cells (Fig. 8, Fig. 9A), suggesting that basolateral membrane polarity was not inverted in the cysts of mLgl kd cells. These data suggest that mLgl knockdown affects the orientation of apical membrane polarity but does not induce an inverted apical-basal polarity phenotype during the early phase of cystogenesis.

Moreover, subsequent cystogenesis and lumen formation were also perturbed in cysts of mLgl kd cells, resulting in the formation of cell aggregates without obvious lumens (Fig. 9A, days 5-7). Quantification analysis of day 7 cysts revealed that approximately 80% of cysts of both mLgl kd cells (#1 and #2) establish cell aggregates without obvious lumens, whereas only 20% of control cysts established cell aggregates (Fig. 9B). Concentrated F-actin staining and distribution of PAR-6β in the inner surfaces of the cysts were affected by mLgl knockdown (Fig. 9A,C), suggesting that the establishment of apical lumens was disorganized in cysts of mLgl kd cells. These data imply that the mLgl-mediated orientation of apical membrane polarity seems to be one of the important steps for lumen formation during cystogenesis. We further revealed that the overexpression of PAR-3 showed a similar phenotype to that of mLgl kd knockdown; approximately 80% of PAR-3-expressing cysts formed cell aggregates without lumens (supplementary material Fig. S4). These data further suggest that the regulated counterbalance between mLgl and PAR-3–aPKC–PAR-6 is also important for cystogenesis.

Discussion

This study suggests that in some specific conditions, such as Ca^{2+}-depletion and collagen-gel overlay, mLgl actively suppresses apical PAR-3–aPKC–PAR-6 complex to facilitate the redistribution of apical membrane domains in epithelial cells. Further, analysis of 3D-cultured cells suggests the importance of this mLgl-function for the orientation of apical membrane polarity to create cysts with lumen (Fig. 10).

Analysis of depolarization of MDCK cells suggests that mLgl-mediated disassembly of apical membrane proteins is mediated by the enhancement of internalization of apical proteins. A similar phenomenon has also been observed when the apical membrane polarity in cysts is reversed; that is, when MDCK cysts formed in a suspension culture are placed in a collagen gel, the pre-existing apical membrane domains at outer surface of the cysts are disassembled by internalization,

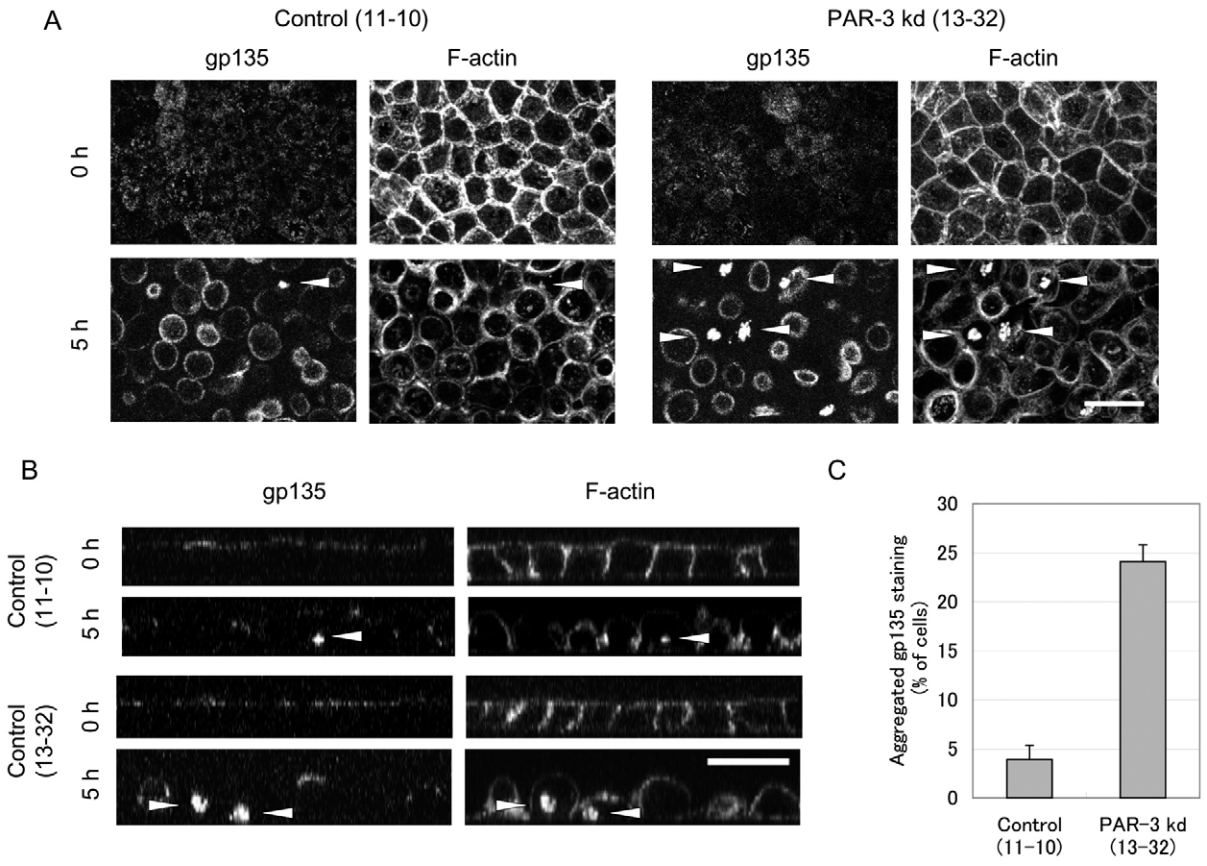

Fig. 5. Knockdown of PAR-3 accelerates disassembly of apical proteins during depolarization of MDCK cells. Confluent monolayers were incubated with gp135 mouse antibody for 1 hour. After washing out the antibody, the cells were incubated with LC medium for the indicated time. The cells were fixed, permeabilized and stained with Alexa Fluor 488-conjugated anti-mouse IgG together with rhodamine-phalloidin. (A) Projected views of optical sections from the apical to the basal membranes of cells. (B) Confocal z-sections. Arrowheads indicate the cells with intracellular gp135 and F-actin staining. (C) Quantification of cells with aggregated gp135 staining after incubation with LC medium for 5 hour. The percentage of total cells is shown. Values are mean (±s.d.) of three independent experiments. Bars, 20 μm.

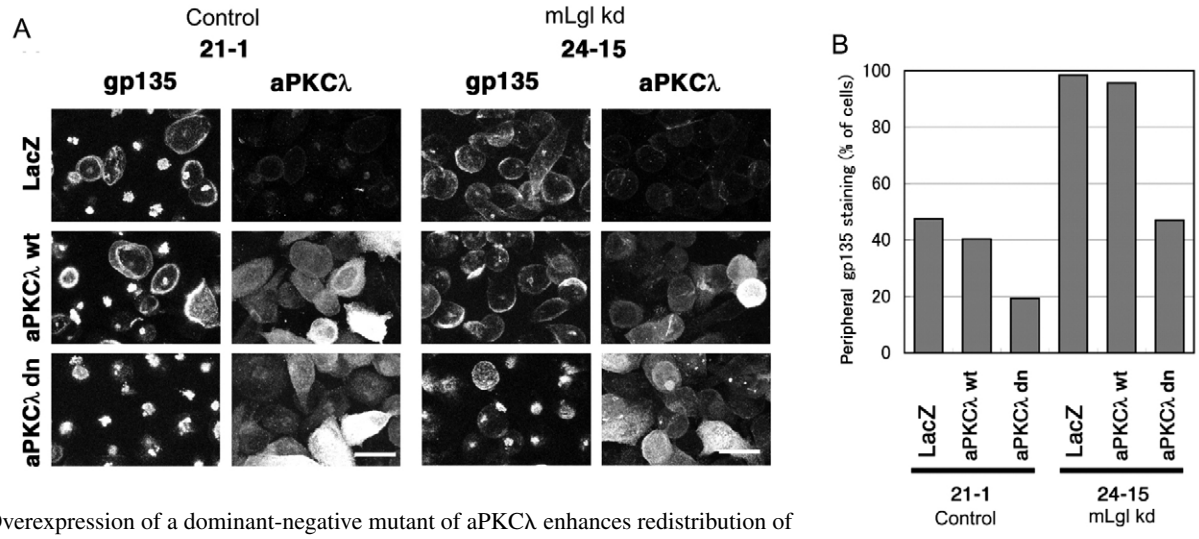

Fig. 6. Overexpression of a dominant-negative mutant of aPKCλ enhances redistribution of gp135 and suppresses phenotype of mLgl knockdown. (A) mLgl kd cells (24-15) or control cells (21-1) on permeable filters were infected with adenovirus expression vectors encoding LacZ, wild-type aPKCλ (aPKCλ wt) or dominant-negative aPKCλ (aPKCλ dn) for 2 hours. The cells were then incubated with LC medium for 18 hours. (A) Cells were fixed and double stained with anti-aPKCλ and anti-gp135 antibodies. Notice that the overexpression of aPKCλ dn but not aPKCλ wt in the control or the mLgl kd cells decreases the peripheral gp135 staining in depolarized cells. (B) Quantification of the cells with cell peripheral gp135 staining in A. Each photograph represents the projected views of confocal sections. Bars, 20 μm.

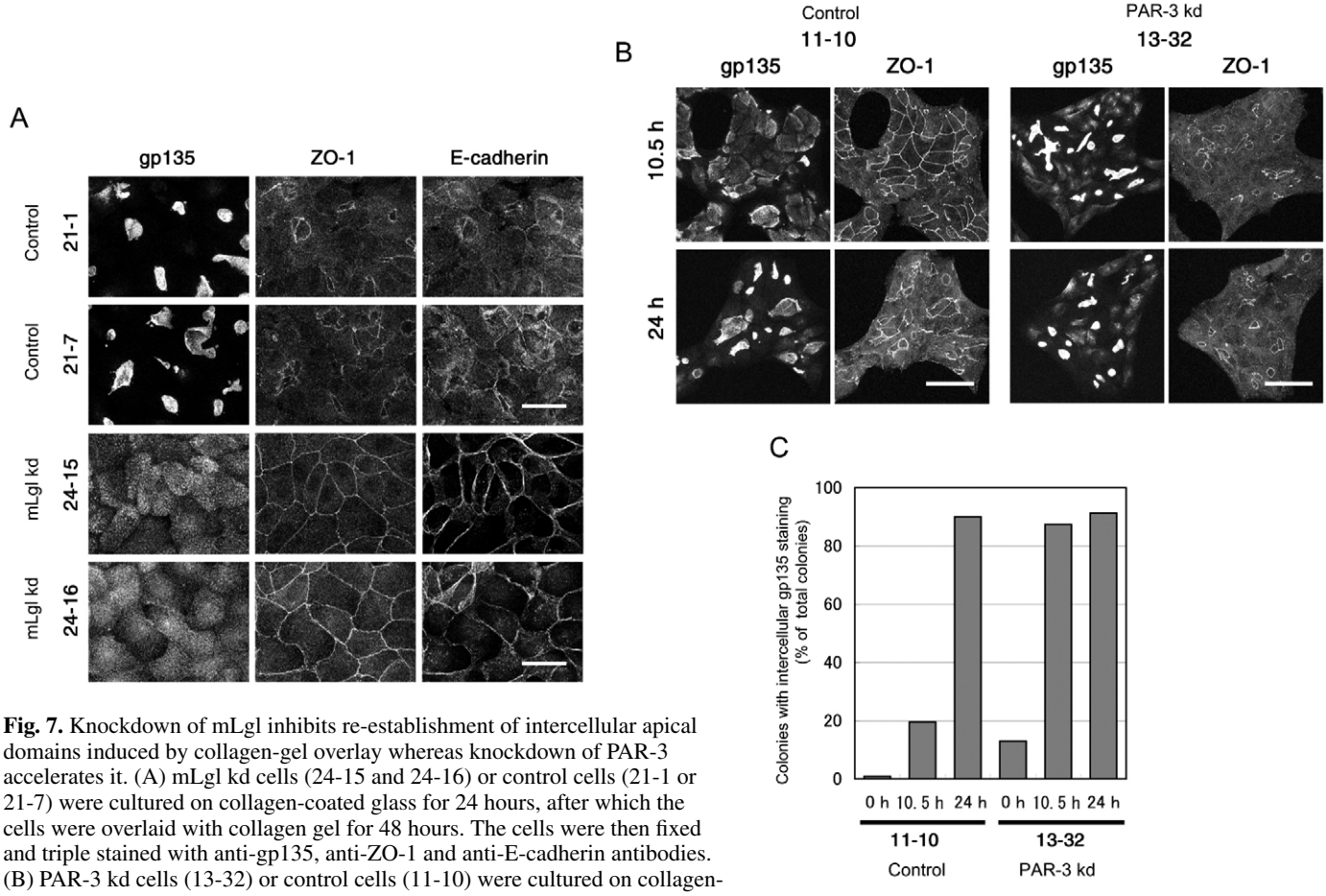

Fig. 7. Knockdown of mLgl inhibits re-establishment of intercellular apical domains induced by collagen-gel overlay whereas knockdown of PAR-3 accelerates it. (A) mLgl kd cells (24-15 and 24-16) or control cells (21-1 or 21-7) were cultured on collagen-coated glass for 24 hours, after which the cells were overlaid with collagen gel for 48 hours. The cells were then fixed and triple stained with anti-gp135, anti-ZO-1 and anti-E-cadherin antibodies. (B) PAR-3 kd cells (13-32) or control cells (11-10) were cultured on collagen-coated glass for 24 hours, after which the cells were overlaid with collagen gel for 10.5 or 24 hours. The cells were fixed and double stained with anti-gp135 and anti-ZO-1 antibodies. (C) Quantification of colonies with concentrated gp135 staining at intercellular regions at indicated times after collagen-gel overlay. Scale bars represent 20 μm. Photographs represent the projected views of confocal sections. Bars, 20 μm (A) or 50 μm (B).

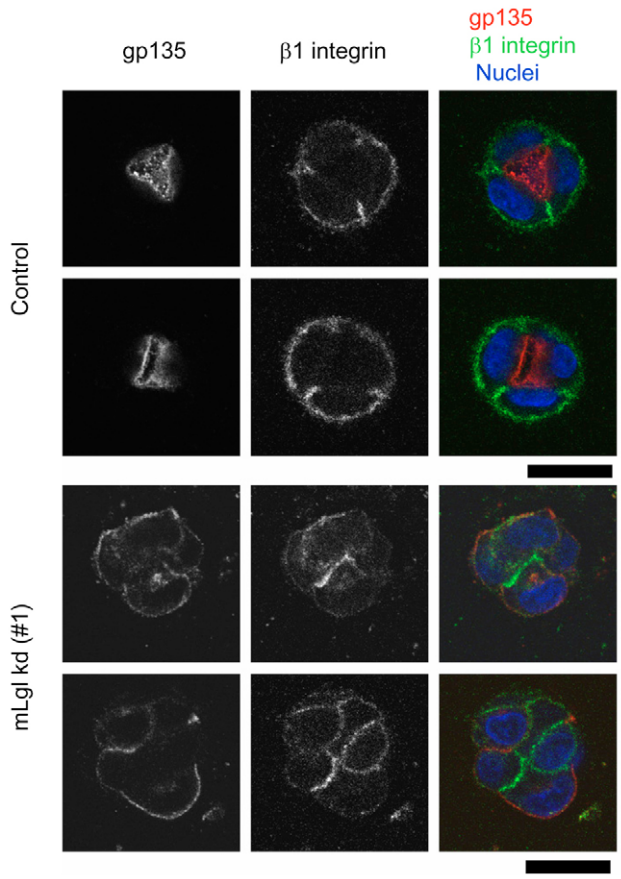

Fig. 8. Knockdown of mLgl mislocalizes apical gp135 to outer surface of cyst where cells face collagen gel at initial stage of cystogenesis. mLgl kd cells (#1) or control cells were suspended in collagen gel and cultured for 2 days. Then, cysts were fixed and stained with anti-gp135 and anti-β1 integrin antibodies. The respective major examples are shown. Notice that gp135 staining was detected at the outer surface of cell aggregates derived from Lgl kd cells, whereas gp135 staining was detected at the inner surface of cell aggregates from control cells. Each photograph represents the single *x-y* confocal section. Bars, 20 μm.

after which new apical domains are formed at the central position of cysts (Wang et al., 1990). Thus, this study suggests that suppressive regulation of the apical PAR-3–aPKC–PAR-6 complex by mLgl is required for collagen-induced disassembly of peripheral apical membrane domains by internalization of apical proteins, through which cells can orient their apical membrane polarity. Interestingly, we found that only an mLgl-2 knockdown showed a similar effect to mLgl-1–mLgl-2 double-knockdown on apical protein localization in depolarized cells (data not shown). This is consistent with our previous observation that mLgl-2 preferentially coimmunoprecipitates with PAR-6 from MDCK cell lysates (Yamanaka et al., 2003), and suggests that the mLgl-2 isoform mainly regulates the apical domain in these cells.

In addition to apical domain disassembly, we showed here that the mLgl knockdown also partially suppressed the disassembly of tight junction proteins induced by Ca^{2+}-depletion. Interestingly, we also found that the localization of one of the adherens junction proteins, E-cadherin, was also affected in mLgl kd cells; that is, E-cadherin accumulation in the interacellular region in depolarizing cells was suppressed in mLgl kd cells (supplementary material Fig. S5A). Thus, it seems that mLgl is involved in the regulation of localization of tight junction and adherens junction proteins in addition to that of apical membrane proteins (Fig. 10). Therefore, does mLgl regulate junction proteins and apical membrane proteins independently or interdependently? The following data suggests that the localization of apical proteins seems to be regulated by mLgl independently of tight junctions and adherens junctions. First, apical proteins were retained at the cell periphery even in highly depolarized cells, in which peripheral ZO-1 staining almost disappeared (Fig. 1). Second, PAR-3 overexpression – showing similar effects to mLgl knockdown on apical protein localization, or PAR-3 knockdown – showing opposite effects to mLgl knockdown, did not show clear effects on E-cadherin localization (supplementary material Fig. S5B,C). The mechanism of mLgl on the regulation of tight junctions and adherens junctions remains obscure and requires further investigations.

This study suggests that the suppression of apical PAR-3–aPKC–PAR-6 complex activity by mLgl is mediated through the suppression of the interaction of the aPKC–PAR-6 complex with PAR-3 or Cdc42. Thus, what are the roles of PAR-3 and Cdc42 in this complex? PAR-3 seems to serve as a scaffold of the aPKC–PAR-6 complex to the cortical region of epithelial cells because, in addition to the apical cortical proteins, a PAR-3 knockdown also accelerates the disappearance of aPKC and PAR-6 from the cell periphery in response to Ca^{2+}-depletion (T.Y. and S.O., unpublished data). By contrast, Cdc42 seems to be involved in the regulation of aPKC activity because Cdc42 activates aPKC through PAR-6 in vitro (Yamanaka et al., 2001). Another possible role of Cdc42 is that it regulates the interaction of the aPKC–PAR-6 complex with another apical protein complex, the CRB3-Pals1 complex (Hurd et al., 2003; Lemmers et al., 2004; Wang et al., 2004). This complex is important for the establishment of apical membrane domains in epithelial cells (Cao et al., 2005; Roh et al., 2003), and Cdc42 has been shown to be required for the interaction between PAR-6 and Pals1 (Hurd et al., 2003). Thus, PAR-3 and Cdc42 seem to have important roles in localization, activity and protein-protein interaction of the aPKC–PAR-6 complex, which are affected by mLgl during the redistribution of apical proteins in epithelial cells (Fig. 10). The second important question is how mLgl regulates the interaction of PAR-6 with Cdc42 in addition to PAR-3. One possible explanation is that mLgl physically competes with Cdc42 for its interaction with PAR-6, because the CRIB region of PAR-6 is located just before the PDZ domain that interacts with mLgl (Yamanaka et al., 2003). Alternatively, mLgl might cause a conformational change in the CRIB-PDZ region of PAR-6 and, consequently, the dissociation of Cdc42 from PAR-6.

Previous studies have suggested that Rac1, which is activated by interaction of integrin with collagen, is also important for the orientation of apical membrane polarity by regulating laminin-ECM organization (O'Brien et al., 2001; Yu et al., 2005). Here, we showed that Cdc42 but not Rac1 was detected in PAR-6-IP from mLgl kd cells, suggesting that aPKC–PAR-6 interacts with Cdc42 rather than Rac1 under the control of mLgl to regulate apical membrane polarity. Consistent with this, recent observation suggests that, in

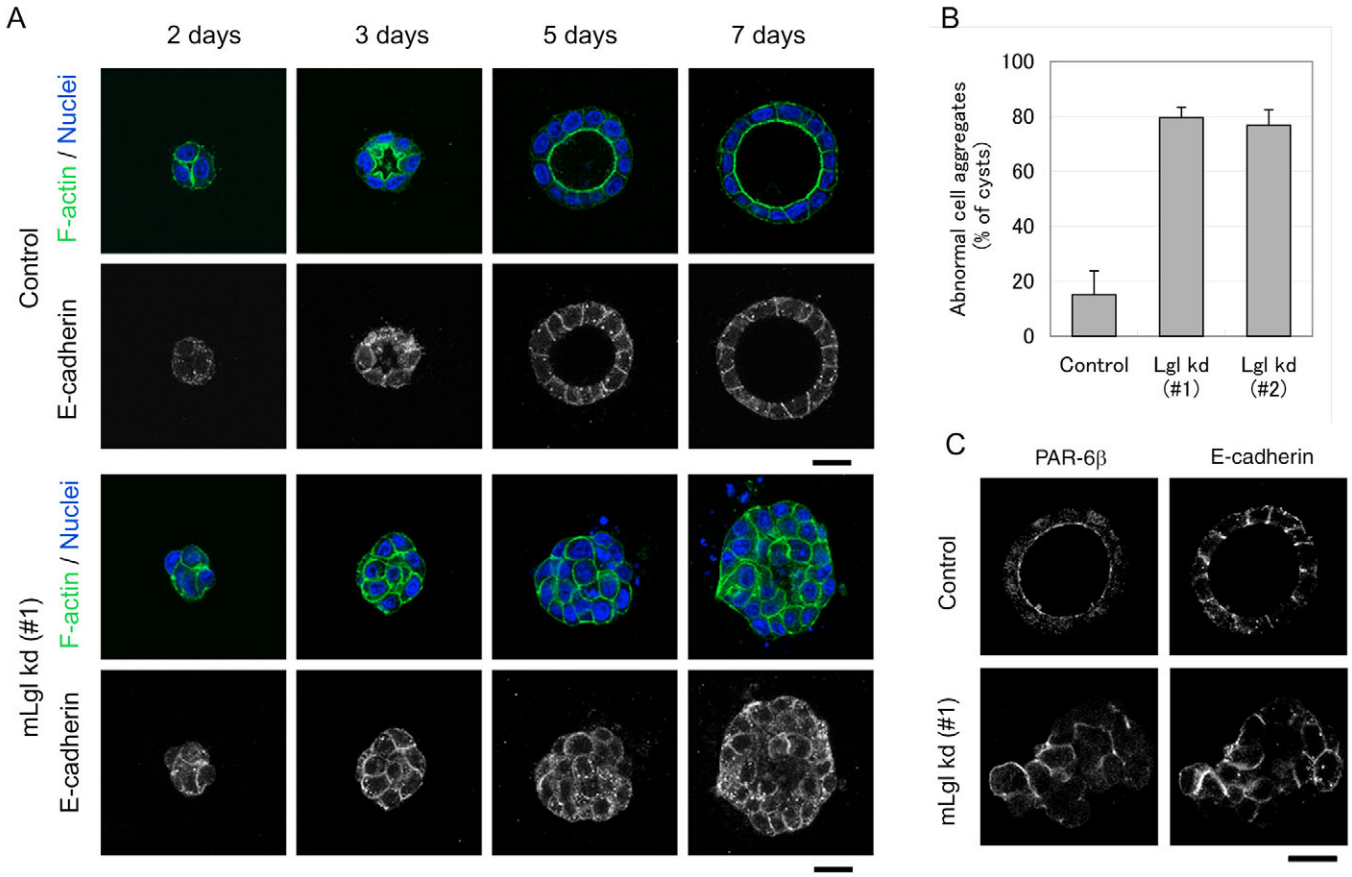

Fig. 9. Knockdown of mLgl induces formation of abnormal cell aggregates without obvious lumens during MDCK cell cystogenesis. (A) mLgl kd cells (#1) or control cells were suspended in collagen gel and cultured for the indicated time. Then cysts were fixed and stained with rhodamine-phalloidin and anti-E-cadherin antibody. Cell nuclei were stained with TOPRO3. Notice that mLgl knockdown affected the actin distribution during cystogenesis, leading to the formation of cell aggregates without lumens. (B) Quantification of abnormal cell aggregates in total cysts at day 7 is shown. Values are the mean (±s.d.) of three independent experiments. Notice that about 80% of cysts of both mLgl kd cells (#1 and #2) formed abnormal cell aggregates. (C) mLgl kd (#1) or control cells were suspended in collagen gel and cultured for 7 days, and then were fixed and stained with anti-PAR-6β and anti-E-cadherin antibodies. Notice that the distribution of PAR-6β to the inner surfaces of the cysts was affected in cysts of mLgl kd cells. Each photograph represents the confocal single *x*-*y* section. Bars, 20 μm.

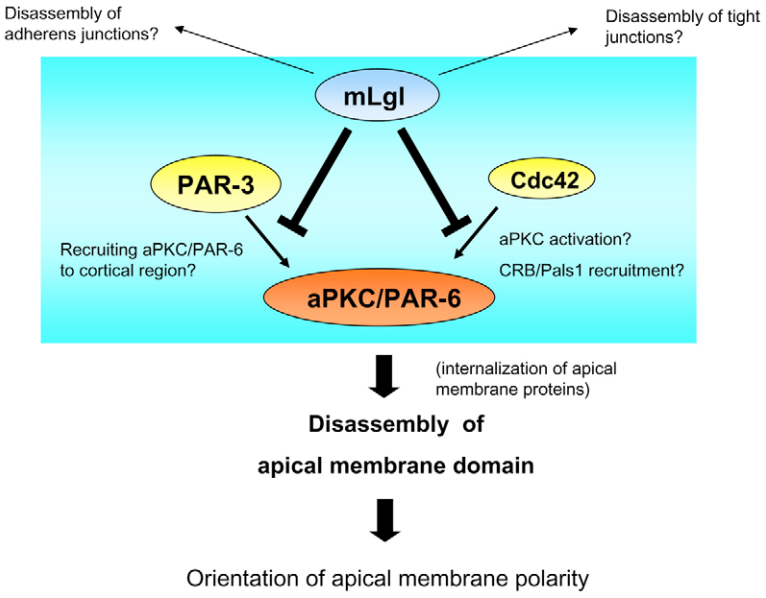

Fig. 10. Schematic model of mechanism of mLgl-mediated disassembly of apical domain by suppressing PAR-3–aPKC–PAR-6 complex activity. mLgl suppresses the activity of PAR-3–aPKC–PAR-6 complex by the competitive interaction of aPKC–PAR-6 with PAR-3 and Cdc42. This leads to the disassembly of the apical membrane domain by internalization of apical proteins and orientation of apical membrane polarity. mLgl seems to also be involved in the regulation of tight junction and adherens junction disassembly.

addition to Rac1, Cdc42 is also involved in the regulation of apical membrane polarity in cysts, that is, the overexpression of a dominant-negative mutant of Cdc42 induces a polarity reversal phenotype in cysts (Rogers et al., 2003). Thus, in addition to the integrin-Rac1 pathway, mLgl-mediated inhibition of the interaction of the apical protein complex with Cdc42 seems to be one of several important pathways influencing the orientation of apical membrane polarity.

In epithelial tissues, the axis of each polarized epithelial cell must be aligned with the overall structure of the tissue to achieve a specific architecture. This study suggests the intriguing possibility that mLgl functions as a mediator of cell adhesion stimuli to create a corresponding apical membrane domain and lumen during epithelial tissue morphogenesis. This can be one of several mechanisms that integrate one cell polarization to epithelial tissue morphogenesis. Further studies are needed to obtain deeper insights into the mechanisms underlying the regulation of epithelial tissue morphology.

Materials and Methods

Expression vectors

Adenoviral expression vectors encoding mouse wild-type aPKCλ (aPKCλ wt), a kinase-deficient dominant-negative mutant (aPKCλ dn) and LacZ generated with pAxCAwt were described previously (Suzuki et al., 2001). Adenoviral expression vectors encoding hemagglutinin (HA)-tagged mLgl-2 (HA-mLgl-2) and an empty vector generated with the Adeno-X expression system (Clontech, Palo Alto, CA) were described previously (Yamanaka et al., 2003). cDNA for T7-tagged full-length PAR-3 (1-1337 aa) was subcloned into vector pEB6-CAG, an Epstein-Barr virus (EBV)-based extrachoromosomal vector carrying a replication origin (oriP) and a replication initiation factor (EBNA-1) that are sufficient for autonomous replication in human and canine cells (Tanaka et al., 1999). pEB6-SUPER vector was established by replacing the CAG promoter region of pEB6-CAG vector with the H1 promoter of pSUPER vector as described previously (Suzuki et al., 2004).

Antibodies

Rabbit anti-PAR-6β polyclonal antibody (pAb) (BC31AP), rat anti-PAR-6β pAb (BCR12AP), rabbit anti-mLgl-2 antibodies (N13AP and 100-278 2-3AP), rabbit anti-mLgl-1 pAb (C-2 AP), rabbit anti-PAR-3 pAb (C2-3AP), and rabbit anti-EMK (PAR-1b) pAb (EM1) have been described previously (Yamanaka et al., 2003; Akimoto et al., 1994; Izumi et al., 1998; Suzuki et al., 2004). Mouse anti-gp135 monoclonal antibody (mAb) (3F2) was generously provided by J. D. Nelson (Stanford University, CA). The following commercially available antibodies were also used: mouse anti-aPKCλ (ι) mAb, mouse anti-E-cadherin mAb, mouse anti-Cdc42 (C70820) mAb (Transduction Laboratories, KY); mouse or rabbit anti-ZO-1 mAb (ZYMED Laboratories Inc., CA); rabbit anti-T7 (Omni) pAb, rabbit anti-ezrin pAb, rabbit anti-aPKC (C20) pAb (Santa Cruz, CA); rabbit anti-HA pAb (Bethyl); rat anti-ZO-1 mAb (Chemicon); mouse anti-β-actin mAb, rat anti-uvomorulin (E-cadherin) mAb (Sigma); rabbit anti-PAR-3 pAb, mouse anti-Rac mAb (05-389: Upstate); rat anti-HA mAb (Roche); and rat β1-integrin mAb (A2B2: Hybridoma bank).

Cell culture

Madin-Darby canine kidney (MDCK) II cells were grown in Dulbecco's modified essential medium (DMEM) containing 10% fetal calf serum (FCS), penicillin and streptomycin, at 5% CO_2 atmosphere and constant humidity. For the Ca^{2+}-depletion assay, cells were seeded on Transwell^{TM} filters (12 mm diameter; Corning Coaster Corp., Cambridge, MA) with a pore size of 0.4 μm (3×10^5 cells/cm^2) and grown for 1 or 2 days to produce a confluent monolayer. Cells were washed with PBS twice and incubated in a low-Ca^{2+} (LC) medium containing 5% FCS, 3 μM Ca^{2+}, penicillin and streptomycin for 20 hours. The Ca^{2+}-switch assay was performed by replacing the LC medium with a normal growth medium for these cells. Adenovirus infection was performed as described previously (Suzuki et al., 2001). Briefly, confluent cells were pre-incubated with LC medium for 2 hours; cells were then incubated with 200 μl of the appropriate virus solution, diluted to 3×10^8 pfu/ml in LC medium, for 2 hours. LC medium was prepared as follows: 25 ml of FCS was incubated with 1.25 g of analytical-grade Chelex 100 resin (BIA-RAD) at 4°C for 1 hour to chelate Ca^{2+} ions. Then, FCS was added to 500 ml of Ca^{2+}-free DMEM (GIBCO), after which $CaCl_2$was added to a final concentration 3 μM, together with penicillin-streptomycin and glutamine.

Generation of siRNA clones

pSUPER vector was generously provided by R. Agami (The Netherlands Cancer Institute, Amsterdam, The Netherlands) (Brummelkamp et al., 2002). pSUPER based vectors containing different antibiotics resistant genes were established: pSUPER-neo, which was established using the pEGFP-N3 vector in which the sequence for CMV-EGFP was replaced by the sequence for the H1 promoter of the pSUPER vector; and pSUPER-puro, which was established by insertion of the sequence for PGK and PAC into *Xho*I site of the pSUPER vector. Partial cDNA sequences of canine homologues of mLgl-1, mLgl-2 and PAR-3 were obtained by reverse transcriptase (RT)-PCR of the total RNA of MDCK II cells using a one-step RT-PCR kit (Qiagen) and cloned into the TOPO vector (Invitrogen). To generate mLgl-1–mLgl-2 double knockdown (kd) MDCK cell clones (24-15 and 24-16), mLgl-2 kd cell lines (2-10 and 2-13) were first established by transfection with pSUPER-puro encoding the mLgl-2 shRNA sequence (5′-GATG-AGAGTTTCACACTGC-3′) and selection with puromycin. Then, clone 2-10 was further transfected with pSUPER-neo encoding the mLgl-1 shRNA sequence (5′-GGTGGCACTCTGCAAGTAC-3′) and selected with G418. Control clones (21-1 and 21-7) were established similarly by using pSUPER-puro and pSUPER-neo vectors with a negative control sequence (5′-CAGTCGCGTTTGCGACTGG-3′). Neomycin-resistant PAR-3 kd clones (13-32 and 13-33) were established by transfection with pSUPER-neo encoding the PAR-3 shRNA sequence (5′-GACAGACTGGTAGCAGTGT-3′) and selection with G418. Control clones (11-10 and 25-2) were established similarly by using pSUPER-neo with the negative control sequence. The puromycin-resistant PAR-3 kd clone (25a) was established by the cotransfection with pSUPER-puro encoding the PAR-3 shRNA sequence (5′-CATGGAGATGGAGGAATAC-33′) and pSUPER-puro encoding another PAR-3 shRNA sequence (5′-GAACAGGATGAGGATGGGA-33′). Control clone (1-5) was established similarly using pSUPER-puro vector with the negative control sequence.

Collagen-gel overlay

The collagen-gel overlay assay was performed as previously described (Ojakian et al., 1997). Briefly, MDCK II cells were seeded on coverslips coated with collagen-I (2×10^4 cells/cm^2). After 1 day, cells were overlaid with collagen-I gel containing 10% FCS in DMEM.

Cyst formation

MDCK cell cyst formation was performed as described previously (O'Brien et al., 2001). Briefly, MDCK cells were trypsinized and suspended with ice-cold water containing 2 mg/ml calf skin type-I collagen (Koken, Tokyo, Japan), DMEM, 20 mM HEPES (pH 7.4), and 5% FBS. The resulting suspension was placed on transwell membrane filters (10 mm in diameter, Corning Costar). After the formation of a gel at 37°C, growth medium was added to the wells. The cells were incubated for several days to form cysts in the gel. Two independent mLgl kd cells, #1 and #2, were generated by introducing pEB6-SUPER with mLgl-1 shRNA into the mLgl-2 kd clone 2-10 and 2-13. Control cells were generated by introducing pEB6-SUPER with the negative-control sequence into control clone 1-5. PAR-3-expressing cells were generated with pEB6-CAG-PAR-3 vector as described previously (Suzuki et al., 2004).

Immunoprecipitation and western blot analysis

MDCK II cells were cultured on 10-cm dishes. Cells were suspended in lysis buffer containing 50 mM Tris-HCl at pH 7.4, 150 mM sodium chloride, 10% glycerol, 1% Triton X-100, 1.5 mM magnesium chloride, 1 mM EGTA, 10 mM sodium fluoride, 10 mM $Na^4P^2O^7$, 1 mM Na^3VO^5, 1 mM phenyl methylsulphonyl fluoride, 10 μg/ml leupeptin and 16 μg/ml aprotinin. After centrifugation at 17,610 ***g*** for 30 minutes, the supernatants were subjected to immunoprecipitation with 2 μg of antibody, followed by SDS-PAGE and western blotting as described previously (Suzuki et al., 2001).

Immunofluorescence microscopy

MDCK cells were fixed with 2% paraformaldehyde and stained as described previously (Suzuki et al., 2001). Secondary antibodies were Alexa Fluor 488-conjugated goat anti-rabbit or goat anti-mouse antibodies, Alexa Fluor 647-conjugated goat anti-mouse antibody (Molecular Probes Inc., Eugene, OR), and Cy3-conjugated goat anti-rabbit or goat anti-rat antibodies (Amersham Bioscience). Rhodamine-phalloidin was used to visualize filamentous actin (Molecular Probes). Samples were mounted with Vectashield (Vector Laboratories, Inc.) and viewed using a confocal microscope system (LSM 510; Carl Zeiss, Germany) or a fluorescence microscope (BX40, Olympus) equipped with a CCD camera (Princeton Instruments, Trenton, NJ).

We thank Y. Miwa (Tsukuba University, Japan) for the EBV-based vector, R. Agami (The Netherlands Cancer Institute, Amsterdam, TheNetherlands) for pSUPER, and J. D. Nelson (Stanford University, CA) for the gp135 antibody. This work was supported by grants from the Ministry of Education, Culture, Sports, Science, and Technology of Japan (S.O.), the Japanese Society for the Promotion of Science (S.O.) and the Japanese Science and Technology Agency (S.O.).

References

Akimoto, K., Mizuno, K., Osada, S., Hirai, S., Tanuma, S., Suzuki, K. and Ohno, S. (1994). A new member of the third class in the protein kinase C family, PKC lambda, expressed dominantly in an undifferentiated mouse embryonal carcinoma cell line and also in many tissues and cells. *J. Biol. Chem.* **269**, 12677-12683.

Betschinger, J., Mechtler, K. and Knoblich, J. A. (2003). The Par complex directs asymmetric cell division by phosphorylating the cytoskeletal protein Lgl. *Nature* **422**, 326-330.

Bilder, D. (2004). Epithelial polarity and proliferation control: links from the Drosophila neoplastic tumor suppressors. *Genes Dev.* **18**, 1909-1925.

Bilder, D., Li, M. and Perrimon, N. (2000). Cooperative regulation of cell polarity and growth by Drosophila tumor suppressors. *Science* **289**, 113-116.

Brummelkamp, T. R., Bernards, R. and Agami, R. (2002). A system for stable expression of short interfering RNAs in mammalian cells. *Science* **296**, 550-553.

Cao, X., Ding, X., Guo, Z., Zhou, R., Wang, F., Fog, V., Long, F., Bi, F., Fan, D., Forte, J. G. et al. (2005). PALS1 specifies the localization of ezrin to the apical membrane of gastric parietal cells. *J. Biol. Chem.* **280**, 13584-13592.

Chalmers, A. D., Pambos, M., Mason, J., Lang, S., Wylie, C. and Papalopulu, N. (2005). aPKC, Crumbs3 and Lgl2 control apicobasal polarity in early vertebrate development. *Development* **132**, 977-986.

Chen, X. and Macara, I. G. (2005). Par-3 controls tight junction assembly through the Rac exchange factor Tiam1. *Nat. Cell Biol.* **7**, 262-269.

Gao, L., Joberty, G. and Macara, I. G. (2002). Assembly of epithelial tight junctions is negatively regulated by Par6. *Curr. Biol.* **12**, 221-225.

Gateff, E. (1978). Malignant neoplasms of genetic origin in Drosophila melanogaster. *Science* **200**, 1448-1459.

Gilbert, T. and Rodriguez-Boulan, E. (1991). Induction of vacuolar apical compartments in the Caco-2 intestinal epithelial cell line. *J. Cell Sci.* **100**, 451-458.

Hirose, T., Izumi, Y., Nagashima, Y., Tamai-Nagai, Y., Kurihara, H., Sakai, T., Suzuki, Y., Yamanaka, T., Suzuki, A., Mizuno, K. et al. (2002). Involvement of ASIP/PAR-3 in the promotion of epithelial tight junction formation. *J. Cell Sci.* **115**, 2485-2495.

Hurd, T. W., Fan, S., Liu, C. J., Kweon, H. K., Hakansson, K. and Margolis, B. (2003). Phosphorylation-dependent binding of 14-3-3 to the polarity protein Par3 regulates cell polarity in mammalian epithelia. *Curr. Biol.* **13**, 2082-2090.

Hutterer, A., Betschinger, J., Petronczki, M. and Knoblich, J. A. (2004). Sequential roles of Cdc42, Par-6, aPKC, and Lgl in the establishment of epithelial polarity during Drosophila embryogenesis. *Dev. Cell* **6**, 845-854.

Izumi, Y., Hirose, T., Tamai, Y., Hirai, S., Nagashima, Y., Fujimoto, T., Tabuse, Y., Kemphues, K. J. and Ohno, S. (1998). An atypical PKC directly associates and colocalizes at the epithelial tight junction with ASIP, a mammalian homologue of Caenorhabditis elegans polarity protein PAR-3. *J. Cell Biol.* **143**, 95-106.

Joberty, G., Petersen, C., Gao, L. and Macara, I. G. (2000). The cell-polarity protein Par6 links Par3 and atypical protein kinase C to Cdc42. *Nat. Cell Biol.* **2**, 531-539.

Klezovitch, O., Fernandez, T. E., Tapscott, S. J. and Vasioukhin, V. (2004). Loss of cell polarity causes severe brain dysplasia in Lgl1 knockout mice. *Genes Dev.* **18**, 559-571.

Knust, E. and Bossinger, O. (2002). Composition and formation of intercellular junctions in epithelial cells. *Science* **298**, 1955-1959.

Lemmers, C., Michel, D., Lane-Guermonprez, L., Delgrossi, M. H., Medina, E., Arsanto, J. P. and Le Bivic, A. (2004). CRB3 binds directly to Par6 and regulates the morphogenesis of the tight junctions in mammalian epithelial cells. *Mol. Biol. Cell* **15**, 1324-1333.

Lin, D., Edwards, A. S., Fawcett, J. P., Mbamalu, G., Scott, J. D. and Pawson, T. (2000). A mammalian PAR-3-PAR-6 complex implicated in Cdc42/Rac1 and aPKC signalling and cell polarity. *Nat. Cell Biol.* **2**, 540-547.

Macara, I. G. (2004). Par proteins: partners in polarization. *Curr. Biol.* **14**, R160-R162.

Mizuno, K., Suzuki, A., Hirose, T., Kitamura, K., Kutsuzawa, K., Futaki, M., Amano, Y. and Ohno, S. (2003). Self-association of PAR-3-mediated by the conserved N-terminal domain contributes to the development of epithelial tight junctions. *J. Biol. Chem.* **278**, 31240-31250.

Muller, H. A. and Wieschaus, E. (1996). armadillo, bazooka, and stardust are critical for early stages in formation of the zonula adherens and maintenance of the polarized blastoderm epithelium in Drosophila. *J. Cell Biol.* **134**, 149-163.

Musch, A., Cohen, D., Yeaman, C., Nelson, W. J., Rodriguez-Boulan, E. and Brennwald, P. J. (2002). Mammalian homolog of Drosophila tumor suppressor lethal (2) giant larvae interacts with basolateral exocytic machinery in Madin-Darby canine kidney cells. *Mol. Biol. Cell* **13**, 158-168.

O'Brien, L. E., Jou, T. S., Pollack, A. L., Zhang, Q., Hansen, S. H., Yurchenco, P. and Mostov, K. E. (2001). Rac1 orientates epithelial apical polarity through effects on basolateral laminin assembly. *Nat. Cell Biol.* **3**, 831-838.

O'Brien, L. E., Zegers, M. M. and Mostov, K. E. (2002). Opinion: building epithelial architecture: insights from three-dimensional culture models. *Nat. Rev. Mol. Cell Biol.* **3**, 531-537.

Ohno, S. (2001). Intercellular junctions and cellular polarity: the PAR-aPKC complex, a conserved core cassette playing fundamental roles in cell polarity. *Curr. Opin. Cell Biol.* **13**, 641-648.

Ohshiro, T., Yagami, T., Zhang, C. and Matsuzaki, F. (2000). Role of cortical tumour-suppressor proteins in asymmetric division of Drosophila neuroblast. *Nature* **408**, 593-596.

Ojakian, G. K., Nelson, W. J. and Beck, K. A. (1997). Mechanisms for de novo biogenesis of an apical membrane compartment in groups of simple epithelial cells surrounded by extracellular matrix. *J. Cell Sci.* **110**, 2781-2794.

Ojakian, G. K., Ratcliffe, D. R. and Schwimmer, R. (2001). Integrin regulation of cell-cell adhesion during epithelial tubule formation. *J. Cell Sci.* **114**, 941-952.

Peng, C. Y., Manning, L., Albertson, R. and Doe, C. Q. (2000). The tumour-suppressor genes lgl and dlg regulate basal protein targeting in Drosophila neuroblasts. *Nature* **408**, 596-600.

Petronczki, M. and Knoblich, J. A. (2001). DmPAR-6 directs epithelial polarity and asymmetric cell division of neuroblasts in Drosophila. *Nat. Cell Biol.* **3**, 43-49.

Rogers, K. K., Jou, T. S., Guo, W. and Lipschutz, J. H. (2003). The Rho family of small GTPases is involved in epithelial cystogenesis and tubulogenesis. *Kidney Int.* **63**, 1632-1644.

Roh, M. H., Fan, S., Liu, C. J. and Margolis, B. (2003). The Crumbs3-Pals1 complex participates in the establishment of polarity in mammalian epithelial cells. *J. Cell Sci.* **116**, 2895-2906.

Rolls, M. M., Albertson, R., Shih, H. P., Lee, C. Y. and Doe, C. Q. (2003). Drosophila aPKC regulates cell polarity and cell proliferation in neuroblasts and epithelia. *J. Cell Biol.* **163**, 1089-1098.

Schwimmer, R. and Ojakian, G. K. (1995). The alpha 2 beta 1 integrin regulates collagen-mediated MDCK epithelial membrane remodeling and tubule formation. *J. Cell Sci.* **108**, 2487-2498.

Suzuki, A., Yamanaka, T., Hirose, T., Manabe, N., Mizuno, K., Shimizu, M., Akimoto, K., Izumi, Y., Ohnishi, T. and Ohno, S. (2001). Atypical protein kinase C is involved in the evolutionarily conserved par protein complex and plays a critical role in establishing epithelia-specific junctional structures. *J. Cell Biol.* **152**, 1183-1196.

Suzuki, A., Ishiyama, C., Hashiba, K., Shimizu, M., Ebnet, K. and Ohno, S. (2002). aPKC kinase activity is required for the asymmetric differentiation of the premature junctional complex during epithelial cell polarization. *J. Cell Sci.* **115**, 3565-3573.

Suzuki, A., Hirata, M., Kamimura, K., Maniwa, R., Yamanaka, T., Mizuno, K., Kishikawa, M., Hirose, H., Amano, Y., Izumi, N. et al. (2004). aPKC acts upstream of PAR-1b in both the establishment and maintenance of mammalian epithelial polarity. *Curr. Biol.* **14**, 1425-1435.

Tanaka, J., Miwa, Y., Miyoshi, K., Ueno, A. and Inoue, H. (1999). Construction of Epstein-Barr virus-based expression vector containing mini-oriP. *Biochem. Biophys Res. Commun.* **264**, 938-943.

Vega-Salas, D. E., Salas, P. J. and Rodriguez-Boulan, E. (1987). Modulation of the expression of an apical plasma membrane protein of Madin-Darby canine kidney epithelial cells: cell-cell interactions control the appearance of a novel intracellular storage compartment. *J. Cell Biol.* **104**, 1249-1259.

Vega-Salas, D. E., Salas, P. J. and Rodriguez-Boulan, E. (1988). Exocytosis of vacuolar apical compartment (VAC): a cell-cell contact controlled mechanism for the establishment of the apical plasma membrane domain in epithelial cells. *J. Cell Biol.* **107**, 1717-1728.

Wang, A. Z., Ojakian, G. K. and Nelson, W. J. (1990). Steps in the morphogenesis of a polarized epithelium. I. Uncoupling the roles of cell-cell and cell-substratum contact in establishing plasma membrane polarity in multicellular epithelial (MDCK) cysts. *J. Cell Sci.* **95**, 137-151.

Wang, Q., Hurd, T. W. and Margolis, B. (2004). Tight junction protein Par6 interacts with an evolutionarily conserved region in the amino terminus of PALS1/stardust. *J. Biol. Chem.* **279**, 30715-30721.

Wodarz, A., Ramrath, A., Grimm, A. and Knust, E. (2000). Drosophila atypical protein kinase C associates with Bazooka and controls polarity of epithelia and neuroblasts. *J. Cell Biol.* **150**, 1361-1374.

Yamanaka, T., Horikoshi, Y., Suzuki, A., Sugiyama, Y., Kitamura, K., Maniwa, R., Nagai, Y., Yamashita, A., Hirose, T., Ishikawa, H. et al. (2001). PAR-6 regulates aPKC activity in a novel way and mediates cell-cell contact-induced formation of the epithelial junctional complex. *Genes Cells* **6**, 721-731.

Yamanaka, T., Horikoshi, Y., Sugiyama, Y., Ishiyama, C., Suzuki, A., Hirose, T., Iwamatsu, A., Shinohara, A. and Ohno, S. (2003). Mammalian Lgl forms a protein complex with PAR-6 and aPKC independently of PAR-3 to regulate epithelial cell polarity. *Curr. Biol.* **13**, 734-743.

Yu, W., Datta, A., Leroy, P., O'Brien, L. E., Mak, G., Jou, T. S., Matlin, K. S., Mostov, K. E. and Zegers, M. M. (2005). Beta1-integrin orients epithelial polarity via Rac1 and laminin. *Mol. Biol. Cell* **16**, 433-445.